

Contact Angles of Thin Liquid Films: Interferometric Determination

A.S. DIMITROV¹, P.A. KRALCHEVSKY¹, A.D. NIKOLOV^{1,*} and DARSH T. WASAN²

¹*Laboratory of Thermodynamics and Physico-Chemical Hydrodynamics University of Sofia,
Faculty of Chemistry, Sofia 1126 (Bulgaria)*

²*Department of Chemical Engineering, Illinois Institute of Technology, Chicago, IL 60616
(U.S.A.)*

(Received 6 June 1989; accepted 29 November 1989)

ABSTRACT

A general method for calculation of three-phase contact angles from interferometric experimental data is proposed. The method is applicable for both usual and differential interferometry. It is specified for the case of horizontal films formed in a cylindrical capillary. The method was tested with model and experimental data for the meniscus profile. In particular, it is found that the contact angle of the meniscus coincides with the contact angle of several different lenses floating in the film. This fact implies that the line tension effect in this case is below the threshold of experimental accuracy.

INTRODUCTION

Contact angles (the angles subtended by three or more interfaces at their line of intersection) are important macroscopic characteristics of a capillary system. These angles, liable to direct measurement, are related by the Neumann-Young equation, and hence they give information about the interfacial tensions and interfacial energy. As shown by Derjaguin [1] and Princen and Mason [2], the contact angle at the periphery of a thin film also accounts for the interaction between the film surfaces. This idea was applied and developed in subsequent studies [3-6].

It should be noted that the contact angle is a purely macroscopic concept. In the real system, sketched in Fig. 1, there is a microscopic transition region between a thin liquid film and the capillary meniscus (the Gibbs-Plateau border), where the film in a microscopic scale gradually changes its thickness. The shape of the meniscus surfaces (away from the transition region) satisfies the known Laplace equation

*To whom correspondence should be addressed.

$$\sigma \left(\frac{1}{R_1} + \frac{1}{R_2} \right) = P_c \quad (1)$$

where σ is the equilibrium surface tension between the two fluid phases, R_1 and R_2 are the two principle radii of curvature at a point on the interface and P_c is the capillary pressure at this point. The profile of the interfaces in the transition region satisfies more complicated equations, accounting for the interaction between the meniscus surfaces (see e.g. Refs [7] and [8]). As illustrated in Fig. 1, the macroscopic contact angle, $2\theta_c$, is subtended by definition between the two *extrapolated* meniscus surfaces, satisfying Eqn (1) [6,7]. Hence the contact angle $2\theta_c$ corresponds to a macroscopic model, representing the film as a membrane of zero thickness (the so-called membrane model). Sometimes it is preferable to use a detailed model, representing the film as a layer of finite thickness h [5]. In particular, the detailed model can be used for the case of very small contact angles, when the membrane model is not applicable, because the extrapolated meniscus surfaces do not intersect (see Refs [9] and [10]). If the meniscus surfaces are not symmetrical (e.g. due to the action of the gravity) two different contact angles, θ_1^h and θ_2^h , correspond to the detailed model (Fig. 1). In this paper we will restrict our considerations to the membrane model when it is applicable.

The simplest way to determine the contact angles (both of thin films and of single interfaces) is to take side-view pictures of the system [11,12]. The major shortcoming of this method is that the region close to the contact line does not appear in the picture, so that the extrapolation of the surfaces until they intersect can be connected with considerable error. This procedure can give correct results if the contact angle is large or if the effects of gravity are neg-

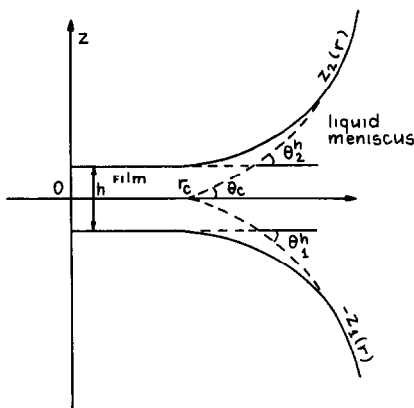


Fig. 1. Sketch of the transition region between a horizontal thin liquid film and the capillary meniscus. The solid and dashed lines represent the real and the extrapolated meniscus profiles, respectively.

ligible and the surfaces are parts of spheres [13,14]. An original modification of this method was developed by Mysels et al. [15,16] for spherical films (at the top of soap bubbles).

Prins [17] and Clint et al. [18] developed a method for macroscopic flat films formed in a glass frame in contact with a bulk liquid. They measured the rise in the force exerted on the film at the moment when the contact angle is formed. Another method was developed by Princen [19] and Princen and Frankel [20], for the same system. They determined the contact angle from the data for diffraction of a laser beam refracted by the liquid meniscus.

In this paper we will focus our attention on the interferometric methods for measurements of contact angles. The main feature of these methods is that the profile of the meniscus surfaces is determined from the data concerning the positions of interference fringes in the liquid meniscus. The fringes are due to differences in the optical paths, Δ , between light beams, reflected (or refracted) by two interfaces. If monochromatic light of wavelength λ is used, the fringes of maximum or minimum intensity (brightness or darkness) are loci of points satisfying the requirement

$$\Delta = i \lambda/2, \quad i=0, 1, 2, \dots, \quad (2)$$

where i is order of interference. There are three different ways to produce interference patterns:

(i) *Usual interferometry (UI)*. This method is illustrated in Fig. 2(a) for the case of a flat thin liquid film. The interference pattern appears when the system is illuminated from above by monochromatic light. The light beams, reflected from the lower meniscus surface $-Z_1(r)$, interfere with the beams reflected from the upper meniscus surface $Z_2(r)$. If n_1 , n_2 and n_3 are the refractive indexes of the three neighboring phases [Fig. 2(a)], then

$$\Delta = 2(Z_1 + Z_2)n_2 \quad (3)$$

When $n_2 > n_1, n_3$, then i in Eqn (2) is odd for the bright and even for the dark fringes. This method was used in Refs [21–27].

(ii) *Differential interferometry in reflected light (DIRL)*. The basic principle of differential interferometry consists of splitting the original image into two images [28,29]. In the so-called shearing method only horizontal splitting is used, so that the two images are shifted at a distance d [Fig. 2(b)]. In the DIRL method each fringe is created by the interference of two beams, *reflected* by the surfaces $Z_2(r, r')$ and $Z'_2(r, r')$ with the same r and r' . Then

$$\Delta = 2(Z_2 - Z'_2)n_3 \quad (4)$$

and i is odd for the dark fringes and even for the bright ones. This method was used in Refs [30] and [31].

(iii) *Differential interferometry in transmitted light (DITL)*. In this case

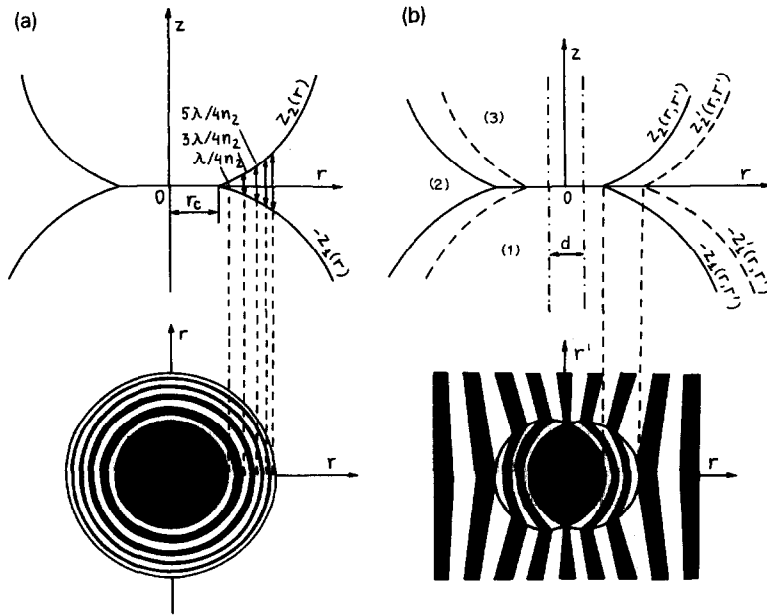


Fig. 2. Section of the reflecting interfaces (upper part of the figure) and sketch of the resulting interference pattern (lower part) for the cases of usual interferometry (a) and differential interferometry (b).

each fringe is created by the interference of two beams, *refracted* by the surfaces $Z_2(r, r')$ and $Z'_2(r, r')$ with the same r and r' [Fig. 2(b)]. Then

$$\Delta = n_2 [(Z_2 + Z_1) - (Z'_2 + Z'_1)] - n_1 (Z_1 - Z'_1) - n_3 (Z_2 - Z'_2) \quad (5)$$

and i is odd for the dark fringes and even for the bright ones. This method was applied by Zorin [32] and Zorin et al. [33] for flat thin liquid films.

The calculation of the contact angle from the interference pattern is simple only when the interfaces are spherical [22,25–27]. Otherwise the interpretation of the data meets considerable mathematical complications. Scheludko et al. [21] approximated the shape of the meniscus around the contact line [Fig. 2(a)] by a parabola, $Z = A_0 r^2 + A_1 r + A_2$ and determined the constants A_0 , A_1 and A_2 by applying Eqn (3) only to three fringes. A weakness of this method is that such a purely empirical approach, which does not use the Laplace equation, Eqn (1), makes the extrapolation procedure uncertain, as pointed out by Haydon and Taylor [22]. This shortcoming was avoided by Kolarov [34], who developed a method based on an approximate solution of the Laplace equation. A more accurate procedure was proposed by Babak [10].

We formulate below a general approach for interpreting the interference pattern and for calculation of the contact angle based on the exact solution of

the Laplace equation. Then the method is specified for a horizontal thin liquid film in a circular capillary [Fig. 2(a)] and the results are compared with the method of Kolarov [34]. New experimental data for horizontal films containing lenses is proceeded by means of our method for the meniscus and by means of the method of Haydon and Taylor [22] for the lenses, and the results are compared. We hope that the general approach formulated below and its application for a specified system will be helpful for the utilization of the interferometric methods for the large variety of capillary systems.

INTERPRETATION OF THE INTERFERENCE PATTERN

General approach

Let r_i , $i=1,2,\dots,N$, be the location of the i th interference fringe and let ΔZ_i be the thickness of the liquid meniscus on the place of the respective fringe. r_i , $i=1,2,\dots,N$ can be measured directly from the observed interference pattern or from its photograph. For UI a common microscope can be used, whilst a specially designed microscope (e.g. Epival Interphako, Carl Zeiss, Jena [35]) is needed for differential interferometric measurements. ΔZ_i , $i=1,2,\dots,N$, can be calculated from Eqns (3)–(5) depending on the method used. In all cases, $\Delta Z_i \geq \lambda/4n_2 > 100$ nm ($\lambda = 546$ nm). It is expected that for distances greater than 100 nm the interaction between the two meniscus surfaces is negligible, and hence the interferometric data are not affected by the film–meniscus transition region. Then the profile of the meniscus surfaces must satisfy the Laplace equation, Eqn (1), which can be transformed into a second-order differential equation [36] whose solutions for the two meniscus surfaces leads in principle to a theoretical expression for ΔZ_i :

$$\Delta Z_i = \Delta Z(r_i; \alpha_1, \dots, \alpha_k), \quad i=1,2,\dots,N \quad (6)$$

where $\alpha_1, \alpha_2, \dots, \alpha_k$ are several parameters usually connected with the boundary conditions at the contact line. (For example, one of these parameters can be the contact angle, another can be the location of the contact line, etc.) In general, the values of the parameters $\alpha_1, \alpha_2, \dots, \alpha_k$ can be determined from the interferometric data $(r_i, \Delta Z_i)$, $i=1, \dots, N$, by using the least-squares principle, i.e. from the condition that the function

$$\Phi_1(\alpha_1, \dots, \alpha_k) = \sum_{i=1}^N [\Delta Z_i - \Delta Z_i(r_i; \alpha_1, \dots, \alpha_k)]^2 \quad (7)$$

is a minimum.

Usually the experimental error of r_i is greater than the error of ΔZ_i . [The wavelength λ of the monochromatic light in Eqns (3)–(5) is known with great

accuracy.] Then from a statistical viewpoint it is correct to determine $\alpha_1, \alpha_2, \dots, \alpha_k$ from the condition for minimum of the function

$$\Phi_2(\alpha_1, \dots, \alpha_k) = \sum_{i=1}^N [r_i - X_i(\Delta Z_i; \alpha_1, \dots, \alpha_k)]^2 \quad (8)$$

where

$$X_i(\Delta Z_i; \alpha_1, \dots, \alpha_k), i=1, \dots, N \quad (9)$$

is the inverse function of ΔZ in Eqn (6).

As far as we know, the optimization approach (the least-squares principle) was first introduced by Gauss in 1801 for determining the orbital parameters of the asteroid Ceres from data obtained by astronomic observations [46]. With capillary systems this approach was used by Huh and Read [47], and by Rotenberg et al. [48] for the determination of surface tension and contact angles from the shapes of axisymmetric fluid interfaces. The application of the general approach for a specified system is not a trivial problem: one has to develop a method for calculation of the functions Φ_1 , or Φ_2 .

The approach based on Eqn (7) or (8) can be applied to horizontal films (Fig. 2), as well as to spherical films [Figs 3(a) and (b)]. The types of the functions ΔZ in Eqn (6) and X in Eqn (9) depend on the specified capillary system. If these functions are complicated or they are not available in explicit form, the minimization of Φ_1 or Φ_2 with respect to the parameters $\alpha_1, \dots, \alpha_k$ can be carried out numerically. It is expedient to minimize with respect to the least possible number parameters $\alpha_1, \dots, \alpha_k$, eliminating the other parameters of the interfacial profile from the condition for mechanical equilibrium at the contact line [8,13,37,42]:

$$\gamma + \sigma_1 + \sigma_2 + \sigma_\kappa = 0 \quad (10)$$

The above vectorial equation is illustrated in Fig. 3(b): γ , σ_1 and σ_2 act tangentially to the film and the two meniscus surfaces and are equal in magnitude to the film tension γ and the respective surface tensions σ_1 and σ_2 . The force σ_κ is directed to the center of curvature of the contact line and is determined by the line tension κ and the radius of curvature r_c of the contact line: $|\sigma_\kappa| = \kappa/r_c$.

The general approach described for the calculation of contact angles from interferometric data is applied below for a specified system.

Application to horizontal films in a capillary

Let us consider a horizontal thin film surrounded by an axisymmetric liquid meniscus [Fig. 2(a)]. (Such films can be formed experimentally inside a cylindrical capillary [38].) It is convenient to choose the surface of tension of the film to be the XY plane of the coordinate system. Let $Z_1(r)$ and $Z_2(r)$ be

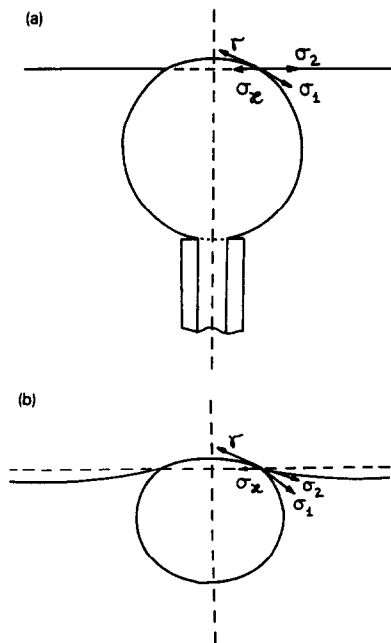


Fig. 3. Sketch of a bubble or drop from a liquid of lower density, attached to an interface. The bubble (drop) can be attached to a capillary [15] (a) or it can be floating [30] (b). The vectors illustrate Eqn (10).

the generatrixes of the two meniscus surfaces; r is the distance to the axis of symmetry (the Z -axis) and both $Z_j(r)$ are positive quantities by definition [Fig. 2(a)]. Then the Laplace equation, Eqn (1), for the two meniscus surfaces can be transformed to read [36]:

$$\sigma \left(\frac{d \sin \theta_j}{dr} + \frac{\sin \theta_j}{r} \right) = P_0 + (-1)^j \Delta \rho g Z_j \quad (11)$$

$$\tan \theta_j = dZ_j/dr, \quad j=1,2 \quad (12)$$

Here $\Delta \rho = \rho_2 - \rho_1 = \rho_2 - \rho_3$ is the difference between the mass densities of phases 2 and 1 (phase 3 being taken as identical to phase 1), g is the acceleration due to gravity, σ is the meniscus surface tension and P_0 is the value of the capillary pressure, P_c , on the level of the film ($Z=0$). Obviously, the last term in Eqn (11) accounts for the contribution of the hydrostatic pressure, and θ_j ($j=1,2$) are running slope angles.

According to the membrane model of the film-meniscus transition region the two meniscus surfaces intersect at the contact line. Hence

$$Z_1(r_c) = Z_2(r_c) = 0 \quad (13)$$

where r_c is the radius of the contact circumference. Besides, if phases 1 and 3 are identical, the vertical projection of the vectorial Eqn (10) reads $\sigma \sin \theta_1(r_c) = \sigma \sin \theta_2(r_c)$, and therefore

$$\theta_1(r_c) = \theta_2(r_c) = \theta_c \quad (14)$$

Equations (13) and (14) serve as boundary conditions for the differential equations (11) and (12).

It is convenient to introduce dimensionless variables

$$x = qr, x_c = qr_c, y_1 = qZ_1, y_2 = qZ_2, P = P_0/q\sigma \quad (15)$$

where the parameter

$$q = (\Delta \rho g / \sigma)^{1/2} \quad (16)$$

has dimension of reverse length. Then Eqns (11)–(14) take the form

$$\frac{ds \sin \theta_j}{dx} + \frac{\sin \theta_j}{x} = P + (-1)^j y_j \quad (17)$$

$$\tan \theta_j = dy_j/dx, j=1,2 \quad (18)$$

$$y_1(x_c) = y_2(x_c) = 0 \quad (19)$$

$$\theta_1(x_c) = \theta_2(x_c) = \theta_c \quad (20)$$

Now it is easy to solve numerically the differential equations (17) and (18) along with the boundary conditions (19) and (20) (e.g. the numerical method proposed by Hartland and Hartley [39] can be used). At given values of x_c , θ_c and P the numerical integration starts from the point $x=x_c$, $y_j=0$ ($j=1,2$). In this way one can calculate the function

$$\Delta y = Y(x; x_c, \theta_c, P) = y_1(x; x_c, \theta_c, P) + y_2(x; x_c, \theta_c, P) \quad (21)$$

determining the dimensionless thickness of the liquid meniscus. The inverse function

$$x = X(\Delta y; x_c, \theta_c, P) \quad (22)$$

expresses the (dimensionalized) distance to the axis of symmetry corresponding to meniscus thickness Δy . Then if

$$\Delta y_i = q \Delta Z_i = i \frac{q \lambda}{4 n_2}, i=1,2,\dots,N \quad (23)$$

are the dimensionalized experimental UI data for the meniscus thickness [cf. Eqns (2), (3) and (16)], the quantities

$$x_i = X(\Delta y_i; x_c, \theta_c, P) \quad (24)$$

will be the calculated theoretical values for the positions of the interference

fringes. In fact, Eqn (24) is a dimensionalized version of Eqn (9), and it is seen that the parameters $\alpha_1, \dots, \alpha_k$ in Eqn (9) in our case are x_c, θ_c and P . According to the general approach described above, these parameters can be determined by minimization of the function

$$\Phi(x_c, \theta_c, P) = \sum_{i=1}^N [X_i - X(\Delta y_i; x_c, \theta_c, P)] \quad (25)$$

where $(x_i, \Delta y_i)$, $i=1, 2, \dots, N$, are couples of experimental values for the i th fringe [cf. Eqn (8)]. In order to start the minimization procedure a zeroth-order approximation $(x_c^{(0)}, \theta_c^{(0)}, P^{(0)})$ for the parameters (x_c, θ_c, P) is needed. Let R be the radius of the capillary in which the film is formed, and let $r_c^{(0)}$ be an approximate estimate of r_c ($r_c^{(0)}$ should be placed somewhere between the first interference fringe and the film of uniform degree of darkness). Then one can use for the zeroth-order approximation the values $x_c^{(0)} = qr_c^{(0)}$, $\theta_c^{(0)} = \arcsin(r_c^{(0)}/R)$ and $P^{(0)} = 2/(qR)$. Another method for obtaining a very accurate zeroth-order approximation for small angles (in the case of UI or DIRL) is described in Appendix I. The error in the values of x_c , θ_c and P thus found, which is due to the random experimental error of the data for x_i in Eqn (25), can be estimated as explained in Appendix II.

We carried out the minimization of $\Phi(x_c, \theta_c, P)$ in Eqn (25) by using the Hooke-Jeeves method [44, 49]. This numerical method consists of the following. Steps of appropriate initial length Δx_c , $\Delta \theta_c$ and ΔP are chosen along the three axes in the space of the variables x_c , θ_c and P . In this way a three-dimensional rectangular lattice of constants Δx_c , $\Delta \theta_c$ and ΔP is defined. Then the

TABLE 1

Three sets of ideal "experimental" data for $r_i = x_i/q$ and $\Delta Z_i = \Delta y_i/q$. The values of $r_c = x_c/q$ and $P_0 = q\sigma P$ are the same for the three sets: $r_c = 20 \mu\text{m}$ and $P_0 = 300 \text{ Pa}$. The values of the other parameters used are: $\sigma = 30 \text{ mN m}^{-1}$, $q = 5.716 \text{ cm}^{-1}$, $\lambda = 0.546 \mu\text{m}$ and $n_2 = 1.334$

i	Set 1: $\theta_c = 0.3^\circ$		Set 2: $\theta_c = 1^\circ$		Set 3: $\theta_c = 10^\circ$	
	$r_i (\mu\text{m})$	$\Delta Z_i (\mu\text{m})$	$r_i (\mu\text{m})$	$\Delta Z_i (\mu\text{m})$	$r_i (\mu\text{m})$	$\Delta Z_i (\mu\text{m})$
1	22.796	0.10232	21.957	0.10232	20.290	0.10232
2	24.187	0.20465	23.238	0.20465	20.579	0.20465
3	25.274	0.30697	24.275	0.30697	20.867	0.30697
4	26.202	0.40929	25.173	0.40929	21.155	0.40929
5	27.028	0.51162	25.980	0.51162	21.441	0.51162
6	27.780	0.61394	26.718	0.61394	21.727	0.61394
7	28.477	0.71627	27.405	0.71627	22.012	0.71627
8	29.129	0.81859	28.050	0.81859	22.296	0.81859
9	29.745	0.92092	28.660	0.92092	22.580	0.92092
10	30.330	1.02324	29.241	1.02324	22.862	1.02324
11	30.889	1.12556	29.797	1.12556	23.143	1.12556

values of $\Phi(x_c, \theta_c, P)$ in the initial point (the zeroth approximation) and in its nearest neighbors in the lattice are calculated. By comparison of these values one can determine the direction of faster decrease of $\Phi(x_c, \theta_c, P)$, as explained in Refs [44 and 49]. Then a step is made in this direction and the behavior of $\Phi(x_c, \theta_c, P)$ in the neighboring lattice points is studied again. The procedure is repeated until a minimum value of Φ is found (the path from the initial point to the point of minimum Φ follows the trajectory of faster decrease of Φ). Then the steps Δx_c , $\Delta \theta_c$ and ΔP are decreased and the procedure is started again from the point of minimum Φ in order to find the coordinates of this point with higher accuracy. The program is stopped when Δx_c , $\Delta \theta_c$ and ΔP become less than the random experimental error of the respective quantities. The program is quickly convergent (e.g. the processing of the data contained in Table 1 by IBM PC XT takes less than 1 min).

RESULTS AND DISCUSSION

Comparison with model meniscus profiles

A straightforward way to check the method for calculation of the contact angle is the following. At given values of the parameters θ_c , x_c and P_0 one can find by numerical integration the respective solution of Eqns (17) and (18) determining the meniscus profile. This means that the function X in Eqn (22) is found. By using Eqn (23) for Δy_c one can calculate the exact positions, x_i ($i=1, \dots, N$), of the interference fringes. Thus an ideal set of "experimental" data $(x_i, \Delta y_i)$ is provided. The test of the minimization procedure consists of a reconstruction of the meniscus profile from the ideal data $(x_i, \Delta y_i)$, $i=1, \dots, N$, and especially in a comparison of the values of θ_c , x_c and P , characterizing the restored and the original profiles.

Table 1 contains three test sets of ideal "experimental" data; corresponding to three values of the contact angle: $\theta_c = 0.3$, 1 and 10° . (For $\theta_c > 10^\circ$ UI is difficult to apply owing to the very close location of the fringes, and it is expedient to use differential interferometry.) The values of the parameters used to provide the data in Table 1 are typical for foam films formed in a capillary (see e.g. Refs [24] and [34]) and $\lambda = 546$ nm corresponds to the green line of the Hg spectrum.

The values of θ_c , r_c and P_0 , determined by means of minimization procedure from the data in Table 1, are compared with the exact values in Table 2. A comparison is also made with the method of Kolarov [34] for interpreting the interferometric data. This method consists of the following. If the slope of the meniscus surfaces and their gravitational deformation are negligible, one can write

$$\sin \theta_n \approx \tan \theta_n, P \gg y \quad (26)$$

TABLE 2

Comparison of the values of θ_c , r_c and P_0 , calculated by the minimization procedure proposed in this paper and by the method of Kolarov [34], with the exact values of these three parameters for the three test sets in Table 1

Set	Method	θ_c (°)	r_c (μm)	P_0 (Pa)
1	Exact	0.3000	20.00	300.0
	Minimization procedure	0.2996	20.00	300.0
	Kolarov [34]	0.2481	19.93	301.5
2	Exact	1.0000	20.00	300.0
	Minimization procedure	0.9999	20.00	300.0
	Kolarov [34]	0.9862	19.99	301.6
3	Exact	10.0000	20.00	300.0
	Minimization procedure	10.0033	20.00	300.2
	Kolarov [34]	10.1550	20.00	306.6

Then an integration of Eqn (17) along with Eqns (18) and (26) yields [24,34]:

$$x \frac{dy}{dx} \approx \frac{1}{2} Px^2 + B \quad (27)$$

where B is a constant of integration, and $y=y_1=y_2$ owing to neglecting the gravity effect. The integration of Eqn (27) gives

$$y - y(x_1) = \frac{P}{4}(x^2 - x_1^2) + B \ln(x/x_1) \quad (28)$$

where x_1 is the dimensionalized radius of the first fringe. Then

$$Y_i = \frac{P}{2}X_i + B \quad (29)$$

where

$$Y_i = \frac{y(x_i) - y(x_1)}{\ln(x_i/x_1)}, X_i = \frac{x_i^2 - x_1^2}{2\ln(x_i/x_1)}, i=2,3,\dots,N$$

Hence the data for Y_i versus X_i should obey a linear dependence, whose slope and intercept yield the values of P and B . Then x_c is determined by solving the equation

$$y(x_1) + \frac{P}{4}(x_c^2 - x_1^2) + B \ln(x_c/x_1) = 0 \quad (30)$$

and from Eqn (27) one can calculate the contact angle [34]:

$$\theta_c = \arctan \left(\frac{1}{2} P x_c - \frac{B}{x_c} \right) \quad (31)$$

Thus the method of Kolarov provides a simple procedure for calculation of the contact angle of horizontal films at the cost of some approximations. A comparison with the exact values of θ_c , r_c and P_0 in Table 2 shows that the method of Kolarov works very well for ideal "experimental" data, except the case of small contact angles ($\theta_c < 0.3^\circ$).

However, the real experimental data always contain a random error due to the inaccuracies of the measurements. The main sources of random error are the measurements of the positions r_i of the interference fringes of maximum intensity (brightness or darkness).

In order to study a situation closer to the real one we introduced a randomly distributed error into the data for r_i ($i=1,\dots,N$) in Table 1. We used a generator of random quantities and assumed a gaussian distribution of the error with standard deviation $\Delta r_i = 0.02 \mu\text{m}$. The ideal "experimental" data modified in this way are shown in Table 3. These data were also proceeded by using the minimization procedure proposed in the previous section and the procedure of Kolarov [34]. The calculated values of θ_c , r_c and P_0 are compared with the exact values in Table 4. A comparison between Tables 2 and 4 demonstrates that the results of the procedure of Kolarov [34] are more strongly affected by the random error of r_i . We consider that this fact can be explained at least in part by the special role of the first interference fringe in the method of Kolarov [see Eqns (28)–(30)]. Nevertheless, except for very small θ_c ($\theta_c < 0.3^\circ$) the

TABLE 3

The three sets of data in Table 1 modified by introduction of a randomly distributed error in the values of r_i with standard deviation $\Delta r_i = 0.02 \mu\text{m}$

i	Set 1: $\theta_c = 0.3^\circ$		Set 2: $\theta_c = 1^\circ$		Set 3: $\theta_c = 10^\circ$	
	r_i (μm)	ΔZ_i (μm)	r_i (μm)	ΔZ_i (μm)	r_i (μm)	ΔZ_i (μm)
1	22.782	0.10232	21.870	0.10232	20.275	0.10232
2	24.193	0.20465	23.286	0.20465	20.582	0.20465
3	25.262	0.30697	24.307	0.30697	20.862	0.30697
4	26.189	0.40929	25.208	0.40929	21.165	0.40929
5	27.037	0.51162	25.959	0.51162	21.447	0.51162
6	27.768	0.61394	26.678	0.61394	21.742	0.61394
7	28.487	0.71627	27.443	0.71627	22.000	0.71627
8	29.135	0.81859	28.066	0.81859	22.288	0.81859
9	29.732	0.92092	28.595	0.92092	22.593	0.92092
10	30.341	1.02324	29.219	1.02324	22.851	1.02323
11	30.886	1.12556	29.835	1.12556	23.141	1.12556

TABLE 4

Comparison of the values of θ_c , r_c and P_0 , calculated by the minimization procedure proposed in this paper and by the method of Kolarov [34], with the exact values of these three parameters for the three test sets in Table 3

Set	Method	θ_c (°)	r_c (μm)	P_0 (Pa)
1	Exact	0.3000	20.00	300.0
	Minimization procedure	0.2417	19.90	299.9
	Kolarov [34]	0.1134	19.70	301.6
2	Exact	1.0000	20.00	300.0
	Minimization procedure	0.8856	19.87	303.6
	Kolarov [34]	0.5512	19.45	310.6
3	Exact	10.0000	20.00	300.0
	Minimization procedure	9.8038	19.99	355.8
	Kolarov [34]	9.8427	19.98	389.8

method of Kolarov can provide a good zeroth approximation for the general minimization procedure. A method for obtaining a zeroth approximation, valid also for small θ_c , is proposed in Appendix I.

Experiment with a horizontal film containing lenses

To check the interferometric method and the minimization procedure we carried out some experiments with horizontal foam films. The film was formed inside a capillary of inner radius 1.8 mm. We used 0.1 mol l⁻¹ aqueous solution of sodium dodecyl sulfate. The surface tension of the solution was $\sigma=29.9 \text{ mN m}^{-1}$ at the temperature of the experiments, 25°C. Under these conditions $\Delta\rho$ in Eqn (16) was 0.998 g cm⁻¹. The construction of the measurement cell (the one containing the film) was the same as in Ref. [40]. Measures were taken to allow saturation of the vapors around the film and the meniscus. The film was illuminated from above (through the objective of the microscope) by monochromatic light of wavelength $\lambda=546 \text{ nm}$.

The equilibrium thin film (of approximate thickness 5 nm) contains several lenses of radii between 10 and 30 μm (Fig. 4). Owing to the usual interference circular fringes are observed in the meniscus as well as in each lens.

We measured the radii of the first 11 interference rings (both dark and bright) in the meniscus along six different radial directions. The averaged values of these radii are presented in Table 5. Then we processed these data by numerical minimization of the function Φ in Eqn (25) and determined $\theta_c=1.9\pm 0.1^\circ$, $r_c=926.4\pm 0.9 \mu\text{m}$ and $P_c=33\pm 4 \text{ Pa}$ (the errors are estimated as explained in Appendix II).



Fig. 4. A photograph of the usual interference pattern produced by several liquid lenses floating in a horizontal foam film in the vicinity of the circular contact line between the film and the capillary meniscus. The length of a scale division is $10 \mu\text{m}$.

TABLE 5

Data for the radii of the interference rings in the meniscus in Fig. 4, measured by means of a microphotometer

Interference order, i	Fringe radius, $r_i (\mu\text{m})$
1	928.0
2	929.4
3	930.6
4	932.0
5	933.1
6	934.5
7	936.0
8	937.0
9	937.9
10	939.1
11	940.1

To compare the contact angle of the meniscus with the contact angles of the lenses we also measured the radii of the interference rings of five lenses in Fig. 4. Then we determined the contact angle of each lens using the following procedure [41].

An estimate shows that the gravitational deformation of the surfaces of a

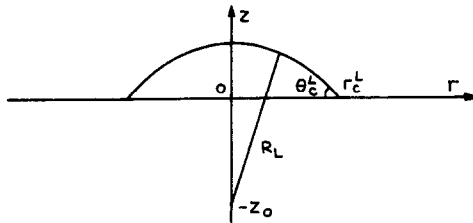


Fig. 5. Section of the spherical upper surface of a lens; Oz is the axis of symmetry; r_c^L and θ_c^L are the radius of the contact line and the contact angle; $-Z_0$ and R_L are the coordinate of the center and the radius of the sphere.

lens is negligible, and hence they are parts of a sphere. The equation of the upper surface of a lens then reads

$$r^2 + (Z + Z_0)^2 = R_L^2 \quad (32)$$

where R_L is the radius of curvature of the lens surface and the other symbols are explained in Fig. 5. The local thickness ΔZ_i of the lens at $r=r_i$ will then be

$$\Delta Z_i = 2(R_L^2 - r_i^2)^{1/2} - 2Z_0 \quad (33)$$

The combination of Eqn (33) with the condition for appearance of an interference fringe, Eqn (23), leads to

$$\frac{i\lambda}{8n_2} = (R_L^2 - r_i^2)^{1/2} - Z_0 \quad (34)$$

From Eqn (34) one derives

$$\frac{k\lambda}{8n_2} = (R_L^2 - r_{i+k}^2)^{1/2} - (R_L^2 - r_i^2)^{1/2}, k \geq 1 \quad (35)$$

Eqn (35) can be transformed to read

$$R_L = \left[r_{i+k}^2 + \left(\frac{4n_2(r_{i+k}^2 - r_i^2)}{k\lambda} - \frac{k\lambda}{16n_2} \right) \right]^{1/2} \quad (36)$$

Then R_L can be calculated for each pair of rings ($i \neq k$). The averaged values of R_L found in this way are presented in Table 6 for the different lenses. Then Z_0 can be calculated from Eqn (34) for each ring. Using the determined mean values of R_L and Z_0 one can calculate the contact radius r_c^L of the lens by setting up $Z=0$ in Eqn (32):

$$r_c^L = (R_L^2 - Z_0^2)^{1/2}$$

Finally, one can calculate the contact angle of the lens

$$\theta_c^L = \arcsin(r_c^L/R_L) \quad (37)$$

TABLE 6

Values of the radius of curvature, R_L , of the contact radius, r_c^L , and of the contact angles, θ_c^L , for five different lenses in Fig. 4

Lens	$R_L \pm 3$ (μm)	$r_c^L \pm 0.1$ (μm)	$\theta_c^L \pm 0.02$ ($^\circ$)
1	588	19.4	1.89
2	607	20.0	1.89
3	673	22.4	1.91
4	838	28.0	1.91
5	879	29.4	1.92

The determined values of r_c^L and θ_c^L are also presented in Table 6. One sees that, in spite of the difference in the contact radii of the lenses, their contact angles coincide in the framework of the experimental accuracy. Hence a line tension effect on the lens contact angle is not detected in this experiment. [Such an effect could in principle exist because of the force balance equation, Eqn (10), whose horizontal projection in this case reads $2\sigma \cos \theta_c^L = \gamma + \kappa/r_c^L$.]

In addition, the contact angles of the lenses, $\theta_c^L = 1.90 \pm 0.02^\circ$, turns out to be in a good agreement with the contact angle of the meniscus, $\theta_c = 1.9 \pm 0.1^\circ$, determined independently from the interference fringes in the meniscus by using the minimization procedure.

CONCLUDING REMARKS

This paper is devoted to the general procedure for the calculation of three-phase contact angles from interferometric data. The theoretical curve determining the profile of the liquid meniscus is in principle known: it is a solution of the Laplace equation, depending on several parameters which are connected with the boundary conditions at the contact line. These parameters (one of them the contact angle) can be determined by fitting the interferometric data to the theoretical curve. According to the least-squares method the condition for best fit is expressed as the condition for a minimum of the functions Φ_1 or Φ_2 defined by Eqns (7) and (8). When the solution of the Laplace equation cannot be expressed analytically, the minimization of the function Φ_1 (or Φ_2) should be carried out numerically along with a numerical solution of the Laplace equation. All available conditions for mechanical equilibrium at the contact line (like Eqn (10) or the buoyancy force equation [42]) must be used to decrease the number of the unknown parameters.

This general approach can be applied both to horizontal films (Fig. 1) and to curved films [Fig. 3(b)]. The interferometric data can be provided by the

usual interference [Fig. 2(a)] as well as by differential interference (in reflected or transmitted light) [Fig. 2(b)].

The minimization procedure was specified for horizontal films formed inside a cylindrical capillary. The method was checked against model data for the meniscus profile, and it turned out that the minimization procedure reproduces the parameters of the profile with a high accuracy. The general method also works well for small contact angles ($\theta_c \leq 0.3^\circ$) where the approximated method of Kolarov can fail. The minimization procedure was also tested for a photograph of a horizontal film containing liquid lenses (Fig. 4). The contact angle of the biconcave meniscus (around the film) calculated by the minimization procedure was in good agreement with the contact angle of the lenses. The latter does not depend on the contact radius of the lenses, which means that the line tension effects in this case are below the threshold of the experimental accuracy.

Summarizing the results of this paper we propose the following scheme for handling interferometric data with horizontal films in a capillary.

(1) The method described in Appendix I is used to calculate the zeroth-order approximation for the contact angle θ_c , the contact radius r_c and the capillary pressure P_0 from the interferometric data.

(2) The gravity deformation of the meniscus is estimated by means of Eqn (A17). If the gravity effect is negligible, then the values of θ_c , r_c and P_0 provided by the zeroth approximation can be regarded as accurate.

(3) If the gravity effect cannot be neglected, the minimization procedure based on Eqn (25) is used to determine θ_c , r_c and P_0 .

(4) The errors in the calculated values of P_0 , r_c and θ_c are determined by Eqns (A19), (A21) and (A22).

It should be noted that in all cases reported in this paper, when we applied the general minimization procedure, the calculated values of θ_c , r_c and P_0 are practically the same as those calculated by the method proposed in Appendix I.

Results for the application of the minimization procedure for floating bubbles, like that in Fig. 3(b), will be soon published [43].

ACKNOWLEDGEMENT

This work was supported in part by the Ministry of Culture, Science and Education of Bulgaria and in part by the U.S. Department of Energy.

APPENDIX I

Zeroth-order approximation for the parameters θ_c , r_c and P_0

The minimization procedure based on Eqn (25) is rapidly convergent if a good zeroth-order approximation is used. We obtained such an approximation in the following way.

In the vicinity of the contact line, where the interference rings are observed, usually $P \gg y_i$ ($i=1,2$). Then an approximate form of Eqn (17) reads

$$\frac{d}{dx}(x \sin \theta) = Px \quad (\text{A1})$$

We omitted the subscript on θ in Eqn (11) because there is no difference between the upper and lower meniscus surfaces when the effect of gravity is neglected. From Eqns (14) and (A1) one easily derives

$$\sin \theta = \frac{1}{2}Px + \frac{Q}{x} \quad (\text{A2})$$

where

$$Q = x_c \sin \theta_c - \frac{1}{2}Px_c \quad (\text{A3})$$

is a constant of integration. Besides, for $\theta \leq 10^\circ$ one can use the equation (with relative error less than 0.0001)

$$\frac{dy}{dx} = \tan \theta \approx \sin \theta + \frac{1}{2} \sin^3 \theta \quad (\text{A4})$$

A substitution from Eqn (A2) in Eqn (A4), followed by integration with respect to x , yields

$$y(x) = \left(\frac{P}{4}\right)^3 (x^4 - x_a^4) + \left(1 + \frac{3}{4}PQ\right) \left(\frac{P}{4}(x^2 - x_a^2) + Q \ln \frac{x}{x_a}\right) + \frac{Q^3}{4} \frac{x^2 - x_a^2}{x^2 x_a^2} + y_a \quad (\text{A5})$$

where $y_a = y(x_a)$. At the contact line $y(x_c) = 0$ and then Eqn (A5) gives

$$\begin{aligned} & \left(\frac{P}{4}\right)^3 (x_c^4 - x_a^4) + \left(1 + \frac{3}{4}PQ\right) \left(\frac{P}{4}(x_c^2 - x_a^2) + Q \ln \frac{x_c}{x_a}\right) \\ & + \frac{Q^3}{4} \frac{x_c^2 - x_a^2}{x_c^2 x_a^2} + y_a = 0 \quad (\text{A6}) \end{aligned}$$

Now let x_a be a given number (we used for x_a a crude preliminary estimate for the contact radius x_c). The dimensionalized local thickness of the meniscus, $\Delta Y = q \Delta Z$, can be expressed as

$$\Delta Y(x; P, Q, y_a) = 2y(x; P, Q, y_a) \quad (\text{A7})$$

Hence ΔY depends on the three unknown constants P , Q and y_a in Eqn (A5). According to Eqn (7) these constants can be determined from the condition for minimum of the function

$$\Phi_1(P, Q, y_a) = \sum_{i=1}^N [\Delta y_i - \Delta Y(x_i; P, Q, y_a)]^2 \quad (\text{A8})$$

where x_i and Δy_i ($i=1, 2, \dots, N$) are experimental data for the interference fringes. ($r_i = x_i/q$ is measured directly and Δy_i is calculated from Eqn (23) at known interference order i .)

A necessary condition for minimum of $\Phi_1(P, Q, y_a)$ is

$$\left(\frac{\partial \Phi_1}{\partial P} \right)_{Q, y_a} = \left(\frac{\partial \Phi_1}{\partial Q} \right)_{P, y_a} = \left(\frac{\partial \Phi_1}{\partial y_a} \right)_{P, Q} = 0 \quad (\text{A9})$$

The substitution of Eqn (A8) in (A9) along with Eqn (23) yields

$$\begin{aligned} \alpha_{11}P + \alpha_{12}Q - \alpha_{13}y_a &= \beta_1 \\ \alpha_{21}P + \alpha_{22}Q + \alpha_{23}y_a &= \beta_2 \\ \alpha_{11}P + \alpha_{12}Q + \alpha_{13}y_a &= \beta_1 \end{aligned} \quad (\text{A10})$$

where

$$\begin{aligned} \alpha_{mn} &= \sum_{i=1}^N f_m(x_i) g_n(x_i), \quad \beta_m = \sum_{i=1}^N \frac{i\lambda}{8n_2} f_m(x_i), \quad m, n = 1, 2, 3 \\ f_1(x_i) &= \frac{3}{4} \left(\frac{P}{4} \right)^2 (x_i^4 - x_a^4) + \frac{1}{4} \left(1 + \frac{3}{2} PQ \right) (x_i^2 - x_a^2) \\ f_2(x_i) &= \left(1 + \frac{3}{2} PQ \right) \ln \frac{x_i}{x_a} + \frac{3Q^2}{4} \frac{x_i^2 - x_a^2}{x_i^2 x_a^2} \\ g_1(x_i) &= \frac{3}{4} \left[\left(\frac{P}{4} \right)^2 (x_i^4 - x_a^4) + \left(1 + \frac{3}{4} PQ \right) (x_i^2 - x_a^2) \right] \\ g_2(x_i) &= \left(1 + \frac{3}{4} PQ \right) \ln \frac{x_i}{x_a} + \frac{Q^2}{4} \frac{x_i^2 - x_a^2}{x_i^2 x_a^2} \\ f_3(x_i) &= g_3(x_i) = 1 \end{aligned} \quad (\text{A11})$$

In spite of the fact that Eqn (A10) has the form of a set of three *linear* equations for the determination of P , Q and y_a , the set (A10) is *not* linear; some of the coefficients α_{mn} and β_m depend on P and Q . To solve the problem we used iterations. At the beginning we set $P = Q = 0$ in Eqn (A11) and then solved Eqn (A10) for P , Q and y_a . The values of P and Q obtained were substituted again into Eqn (A11) and the calculated values of α_{mn} and β_m were used to find the next iteration for P , Q and y_a from Eqn (A10) and so on [10]. With the values of P , Q and y_a determined in this way we calculated x_c and θ_c from Eqns (A3) and (A6).

The above procedure for the determination of θ_c , $r_c = x_c/q$ and $P_0 = \sigma q P$ turned out to be very accurate: for all sets of experimental or model data for r_i and ΔZ_i presented in this paper the procedure based on Eqn (A10) gave the same values of θ_c , r_c and P_0 as the full numerical minimization procedure based on Eqn (25).

APPENDIX II

Effect of gravity and estimation of random errors

An integration of Eqn (17) yields

$$\sin \theta_j = \frac{1}{2}Px + \frac{Q}{x} + (-1)^j \int_{x_c}^x y_j(\zeta) \zeta d\zeta \quad (\text{A12})$$

where q is defined by Eqn (A3). By using $dy_j/dx \approx \sin \theta_j$ as an approximate version of Eqn (18) one derives from Eqns (19) and (A12)

$$y_j(x) = y^{(0)}(x) + y_j^{(g)}(x), j=1,2 \quad (\text{A13})$$

with

$$y^{(0)}(x) = \frac{1}{4}P(x^2 - x_c^2) + Q \ln(x/x_c) \quad (\text{A14})$$

determining the meniscus profile in the absence of gravitational deformation and with

$$y_j^{(g)}(x) = (-1)^j \int_{x_c}^x \frac{dx}{x} \int_{x_c}^x y_j(\zeta) \zeta d\zeta \quad (\text{A15})$$

expressing the effect of gravity on the meniscus shape.

The interference fringes are located between x_c and x_N , where N is the number of the last accounted interference fringe. Hence $x_c < x \leq x_N$ is the domain of interest when dealing with the interferometric data. In view of Eqn (23) one has

$$y_j(x) \leq y_j(x_N) \approx \frac{Nq\lambda}{8n_2} \quad (\text{A16})$$

The substitution of Eqn (A16) into the right-hand side of Eqn (A15) yields

$$y_j^{(g)}(x) = (-1)^j \frac{Nq\lambda}{32n_2} \left(x_N^2 - x_c^2 - 2x_c^2 \ln \frac{x_N}{x_c} \right) \quad (\text{A17})$$

Then the effect of gravity can be estimated by means of the equation

$$\frac{|y_j^{(g)}(x_N)|}{y^{(0)}(x_N)} \leq \frac{Nq\lambda}{8n_2} \frac{x_N^2 - x_c^2 - 2x_c^2 \ln(x_N/x_c)}{P(x_N^2 - x_c^2) + 4Q \ln(x_N/x_c)} \quad (\text{A18})$$

The right-hand side of Eqn (A18) can be calculated by substitution of the values of x_c , P and Q determined by the zeroth-order approximation described in Appendix I.

The three parameters P , Q and y_a satisfy Eqn (A10), and the errors in these parameters can be estimated by means of the standard formulae [45]

$$\Delta P = \left| \frac{A_{11} \Phi_1}{(N-3)D} \right|^{1/2}, \Delta Q = \left| \frac{A_{22} \Phi_1}{(N-3)D} \right|^{1/2}, \Delta y_a = \left| \frac{A_{33} \Phi_1}{(N-3)D} \right|^{1/2} \quad (\text{A19})$$

where Φ_1 is defined according to Eqn (A8), $D = |\alpha_{mn}|$ is the determinant of the set (A10) and

$$A_{11} = \alpha_{22} \alpha_{33} - \alpha_{23} \alpha_{32}, A_{22} = \alpha_{11} \alpha_{33} - \alpha_{13} \alpha_{31}, A_{33} = \alpha_{22} \alpha_{11} - \alpha_{21} \alpha_{12}$$

The substitution $x = x_a$ in Eqn (A14) leads to

$$y_a = \frac{2}{3} P(x_a^2 - x_c^2) + Q \ln(x_a/x_c) \quad (\text{A20})$$

which is an approximate version of Eqn (A6). Equation (A20) can be used to estimate the error in x_c . From Eqn (A20) along with Eqns (15) and (A12) one calculates

$$\frac{\partial x_c}{\partial P} = \frac{x_a^2 - x_c^2}{4 \sin \theta_c}, \frac{\partial x_c}{\partial Q} = \frac{\ln(x_a/x_c)}{\sin \theta_c}, \frac{\partial x_c}{\partial y_a} = \frac{-1}{\sin \theta_c}$$

These expressions, in conjunction with Eqn (A19), determine the error in x_c :

$$\Delta x_c = \Delta(qr_c) = \left[\left(\frac{\partial x_c}{\partial P} \Delta P \right)^2 + \left(\frac{\partial x_c}{\partial Q} \Delta Q \right)^2 + \left(\frac{\partial x_c}{\partial y_a} \Delta y_a \right)^2 \right]^{1/2} \quad (\text{A21})$$

Analogously from Eqn (A3) one determines the error in the contact angle θ_c :

$$\Delta(\sin \theta_c) = \left[\left(\frac{x_c}{2} \Delta P \right)^2 + \left(\frac{\Delta Q}{x_c} \right)^2 + \left(\frac{P}{2} - \frac{Q}{x_c^2} \right)^2 (\Delta x_c)^2 \right]^{1/2} \quad (\text{A22})$$

REFERENCES

- 1 B.V. Derjaguin, Acta Physicochim. URSS, 12 (1940) 181.
- 2 H.M. Princen and S.G. Mason, J. Colloid Sci., 20 (1965) 156.
- 3 J.A. de Feijter, J.B. Rijnbont and A. Vrij, J. Colloid Interface Sci., 64 (1978) 258.
- 4 J.A. de Feijter, in I.B. Ivanov (Ed.), Thin Liquid Films, Marcel Dekker, New York, 1988, p. 1.
- 5 I.B. Ivanov and B.V. Toshev, Colloid Polym. Sci., 253 (1975) 593.

- 6 I.B. Ivanov, B.V. Toshev and B.P. Radoev, in J. Padday (Ed.), *Wetting, Spreading and Adhesion*, Academic Press, London, 1978, p. 37.
- 7 P.A. Kralchevsky and I.B. Ivanov, *Chem. Phys. Lett.*, 121 (1985) 116.
- 8 I.B. Ivanov and P.A. Kralchevsky, in I.B. Ivanov (Ed.), *Thin Liquid Films*, Marcel Dekker, New York, 1988, p. 49.
- 9 A.G. Matynov, I.B. Ivanov and B.V. Toshev, *Kolloidn. Zh.*, 38 (1976) 474.
- 10 V.G. Babak, *Kolloidn. Zh.*, 47 (1985) 582.
- 11 C.A. Smolders and Th.G. Overbeek, *Red. Trav. Chim.*, 80 (1961) 635.
- 12 R.J. Good, in R.J. Good and R.R. Stomberg (Eds.), *Surface and Colloid Science*, Plenum Press, New York, 1979, Vol. 11, p. 1.
- 13 S. Torza and S.G. Mason, *Kolloid. Z. Z. Polym.*, 246 (1971) 593.
- 14 H.M. Princen, M.P. Aronson and J.C. Moser, *J. Colloid Interface Sci.*, 75 (1980) 246.
- 15 H.F. Huisman and K.J. Mysels, *J. Phys. Chem.*, 73 (1969) 486.
- 16 K.J. Mysels, H.F. Huisman and R.L. Razouk, *J. Phys. Chem.*, 70 (1966) 1339.
- 17 A. Prins, *J. Colloid Interface Sci.*, 29 (1969) 177.
- 18 J.H. Clint, J.S. Clunie, J.F. Goodman and J.R. Tate, *Nature (London)*, 223 (1969) 291.
- 19 H.M. Princen, *J. Phys. Chem.*, 72 (1968) 3342.
- 20 H.M. Princen and S. Frankel, *J. Colloid Interface Sci.*, 35 (1971) 186.
- 21 A. Scheludko, B. Radoev and T. Kolarov, *Trans. Faraday Soc.*, 64 (1968) 2213.
- 22 D.A. Haydon and J.L. Taylor, *Nature (London)*, 217 (1968) 739.
- 23 T. Kolarov, *Ann. Univ. Sofia Chim. Fac.*, 66 (1971) 255.
- 24 J.T. Kolarov and Z.M. Zorin, *Kolloidn. Zn.*, 42 (1980) 899.
- 25 Yu.G. Rovin, Ph.D. Thesis, Institute of Inorganic Chemistry, Novosibirsk, 1972 (in Russian).
- 26 P.M. Kruglyakov, Yu.G. Rovin and A.F. Koretskii, *Surface Forces in Thin Films and Stability of Colloids*, Nauka, Moscow, 1974, p. 140 (in Russian).
- 27 P.M. Kruglyakov and Yu.G. Rovin, *Physical Chemistry of Black Hydrocarbon Films*, Nauka, Moscow, 1978 (in Russian).
- 28 M. Francon, *Progress in Microscopy*, Pergamon Press, London, 1961.
- 29 H. Beyer, *Theorie und Praxis der Interferenzmikroskopie*, Akademische Verlagsgesellschaft, Leipzig, 1974.
- 30 A.D. Nikolov, P.A. Kralchevsky and I.B. Ivanov, *J. Colloid Interface Sci.*, 112 (1986) 122.
- 31 A.D. Nikolov, A.S. Dimitrov and P.A. Kralchevsky, *Opt. Acta*, 33 (1986) 1359.
- 32 Z.M. Zorin, *Kolloidn. Zh.*, 39 (1977) 1158.
- 33 Z. Zorin, D. Platikanov, N. Rangelova and A. Scheludko, in B. Derjaguin (Ed.), *Nauka*, Moscow, 1983, p. 200 (in Russian).
- 34 T. Kolarov, *Ann. Univ. Sofia Chim. Fac.*, 73 (1979) 85.
- 35 H. Beyer, *Jenaer Rdsch.*, 16 (1971) 82.
- 36 H.M. Princen, in E. Matijević (Ed.), *Surface and Colloid Science*, Wiley-Interscience, New York, 1969, vol. 2, p. 1.
- 37 A.I. Rusanov, *Phase Equilibria and Surface Phenomena*, Khimia, Leningrad, 1967 (in Russian); *Phasengleichgewichte und Grenzflächenerscheinungen*, Akademie Verlag, Berlin, 1978.
- 38 A. Scheludko, *Adv. Colloid Interface Sci.*, 1 (1967) 391.
- 39 S. Hartland and R.W. Hartley, *Axisymmetric Fluid-Liquid Interfaces*, Elsevier, Amsterdam, 1976.
- 40 A.D. Nikolov and D. Wasan, *J. Colloid Interface Sci.*, 133 (1989) 1.
- 41 A.D. Nikolov, *Ann. High Pedag. School Shoumen*, 88 (1984) 31.
- 42 I.B. Ivanov, P.A. Kralchevsky and A.D. Nikolov, *J. Colloid Interface Sci.*, 112 (1986) 97.
- 43 L.A. Lobo, A.S. Dimitrov, A.D. Nikolov and P.A. Kralchevsky, *Langmuir*, in press.
- 44 B.D. Bunday, *Basic Optimisation Methods*, Edward Arnold, London, 1984.

- 45 A. Sveshnikov, Principles of Error Theory, Leningrad University, Leningrad, 1972 (in Russian).
- 46 G.W. Dunnington, C.F. Gauss: Titan of Science, Hafner, New York, 1955.
- 47 C. Huh and R.L. Reed, *J. Colloid Interface Sci.*, 91 (1983) 472.
- 48 Y. Rotenberg, L. Boruvka and A.W. Neuman, *J. Colloid Interface Sci.*, 93 (1983) 169.
- 49 R. Hooke and T.A. Jeeves, *J. Assoc. Comp. Mach.*, 8 (1961) 212.